ELSEVIER

Biochimica et Biophysica Acta 1510 (2001) 93–105

BIOCHIMICA ET BIOPHYSICA ACTA

BBA

www.elsevier.com/locate/bba

Local anesthetic-induced microscopic and mesoscopic effects in micelles. A fluorescence, spin label and SAXS study

Cilâine V. Teixeira [a], Rosangela Itri [a,*], Fábio Casallanovo [b], Shirley Schreier [b]

[a] *Instituto de Física, Universidade de São Paulo, P.O. Box 66318, São Paulo, SP 05315-970, Brazil*
[b] *Instituto de Química, Universidade de São Paulo, P.O. Box 26077, São Paulo, SP 05513-970, Brazil*

Received 19 June 2000; received in revised form 12 September 2000; accepted 14 September 2000

Abstract

The interaction of the local anesthetic tetracaine (TTC) with anionic sodium lauryl sulfate (SLS) and zwitterionic 3-(*N*-hexadecyl-*N*,*N*-dimethylammonio)propanesulfonate (HPS) micelles was investigated by fluorescence, spin labeling EPR and small angle X-ray scattering (SAXS). Fluorescence pH titrations allowed the choice of adequate pHs for the EPR and SAXS experiments, where either charged or uncharged TTC would be present. The data also indicated that the anesthetic is located in a less polar environment than its charged counterpart in both micellar systems. EPR spectra evidenced that both anesthetic forms increased molecular organization within the SLS micelle, the cationic form exerting a more pronounced effect. The SAXS data showed that protonated TTC causes an increase in the SLS polar shell thickness, hydration number, and aggregation number, whereas the micellar features are not altered upon incorporation of the uncharged drug. The combined results suggest that the electrostatic interaction between charged TTC and SLS, and the intercalation of the drug in the micellar polar region induce a change in molecular packing with a decrease in the mean cross-sectional area, not observed when the neutral drug sinks more deeply into the micellar hydrophobic domain. In the case of HPS micelles, the EPR spectral changes were small for the charged anesthetic and the SAXS data did not evidence any change in micellar structure, suggesting that this species protrudes more into the aqueous phase due to the lack of electrostatic attractive forces in this system.

Keywords: Tetracaine; Micelle; Bilayer; EPR; Fluorescence; Small angle X-ray scattering

1. Introduction

Local anesthetics (LA) are thought to exert their pharmacological action by binding to a specific site at the sodium channel, blocking the action potential [1]. LA also bind to the lipid bilayer, and it has been shown that the more hydrophobic, the more effective [2] and the more toxic the drug [3]. Indeed, LA are able to alter membrane lipid molecular order and/or mobility (for a review, see [4]), to induce [5] or to inhibit [6] the bilayer to hexagonal phase transition, and to promote bilayer to micelle transition [7–9]. These phenomena have been proposed to be involved both in the mechanism of anesthesia [10,11] and in the toxic effects of LA [12–15].

In order to reach their postulated binding site, LA have to cross the lipid bilayer. Most LA are ionizable

* Corresponding author. Fax: +55-11-818-6749; E-mail: itri@if.usp.br

0005-2736/01/$ – see front matter
PII: S0005-2736(00)00338-2

amines and it is widely accepted that the uncharged form traverses the membrane and the ionization equilibrium is reestablished in the cytosol. Moreover, a large body of literature exists showing that both the cationic and neutral forms of LA bind to membranes, and that, in most cases, their binding sites are different, the former being located in the head group region, while the latter sinks more deeply in the acyl chain region (see [4]). Studies with model systems have shown that binding to the membrane modulates physicochemical properties of LA, such as their ionization degree [16–20] and kinetics of reactions [21,22]. Membrane surface charge and ionic strength affect the extent of binding of charged ionizable solutes, and, consequently, their apparent pK (pK_{app}) [19].

However, the effects of LA upon mesoscopic properties of lipid and lipid-like aggregates have not been the object of much investigation. Here, we make use of small angle X-ray scattering (SAXS) experiments performed at the National Laboratory of Synchrotron Light (Brazil) to examine the effects of the charged and uncharged forms of the LA tetracaine (TTC) on the size and shape of negatively charged sodium lauryl sulfate (SLS) and zwitterionic 3-(*N*-hexadecyl-*N*,*N*-dimethylammonio)propanesulfonate (HPS) micelles.

To establish the conditions where either the cationic or the neutral form of the anesthetic would be present, fluorescence titrations were carried out in the presence of micelles. These studies allowed the determination of the binding sites of both forms in the micelles. Information about the location of the binding sites was also obtained from the analysis of the EPR spectral lineshapes of a lipid spin probe incorporated in the micellar aggregates. In addition, the latter analysis provided information about the effects of the anesthetic on the organizational properties within the micelles.

To our knowledge, this is the first study of LA–micelle interaction making use of SAXS.

2. Materials and methods

SLS from Merck, HPS, TTC and the spin label 5-doxyl methyl stearate (5-MeSL), from Sigma, were used without further purification. Deionized and bidistilled water was used throughout. All the experiments were performed at room temperature (21 ± 1°C).

2.1. Fluorescence measurements

Three micromolar TTC was added to samples containing either 1 % (w/w) SLS (35 mM) or HPS (25 mM) in 5 mM phosphate–borate–citrate buffer. The pH varied from 6.0 to 12.0 (SLS) and from 5.0 to 11.0 (HPS). Fluorescence spectra were obtained in a Hitachi F4500 spectrofluorimeter. The excitation wavelength (λ_{ex}) was 302 nm; the spectra were scanned from 310 to 500 nm.

2.2. EPR measurements

The SLS/TTC system was studied at pH 6.5 and 12, to obtain essentially 100% of the charged and uncharged forms of the anesthetic, respectively (see Section 4). The LA concentration varied from 0 to 15 mM. The TTC:surfactant molar ratio (M_{TTC}) varied from 0 to 0.43. For the HPS/TTC system, a pH of 4.5 was used to obtain essentially 100% protonated drug. The anesthetic concentration varied from 0 to 16 mM ($M_{TTC} = 0.64$). Uncharged TTC was not investigated in the presence of HPS micelles, since precipitation occurred at the detergent concentration used. The spin label was incorporated in the micelles at 0.1 mM. EPR spectra were obtained in a Bruker ER200D-SRC spectrometer, operating at the X band (9.5 GHz).

2.3. SAXS measurements

Systems containing 1% (w/w) SLS/water with M_{TTC} varying from 0 to 0.30 (10.5 mM) were studied at pH 6.5 and 12.0, while samples containing 1% (w/w) HPS/water, with $M_{TTC} = 0$ and 0.30 (8.0 mM), were examined at pH 4.5. SAXS experiments were performed at the National Laboratory of Synchrotron Light (LNLS, Campinas, Brazil), with a radiation wavelength of 1.608 Å. The obtained curves were corrected for detector homogeneity and normalized by taking into account the decrease of the intensity of the X-ray beam during the experiment. The parasitic background was subtracted considering a sample's attenuation of 0.25 ± 0.04.

3. Data analysis

3.1. SAXS

It is well known that intermicellar interactions of charged systems exist even at low surfactant volume fractions. In the case of SLS micelles, it has been previously shown [23–25] that, up to a concentration of 10% (w/w) SLS/water, the maximum of the intermicellar interference function falls almost exactly in the region of the minimum of the intramicellar factor in the SAXS curve. As a consequence, the latter presents a peak which is dominated by the detailed form of the micelle. Interference effects start to become important in the SAXS curves only at 15% (w/w) SLS [23,25]. Accordingly, the scattering curves can be analyzed through the distance distribution and the electron distribution functions, which allow the evaluation of the micelle maximum dimension and symmetry as well as details of its inner structure as the mean polar head electron density and the transition between the non-polar and the hydrated polar head regions. In the current work, the results were analyzed by using the Indirect Transformation Process (ITP program) developed by Glatter [26,27], as used in [24,25]. The method consists in determining the distance distribution function $p(r)$ obtained through the fitting of its Fourier transform (convoluted with the beam geometry) to the experimental intensity, according to:

$$I(q) = 4\pi \int_0^{D_{\max}} p(r)\frac{\sin(qr)}{qr}\mathrm{d}r, \quad (1)$$

where $p(r) = r^2\Delta\rho^2(r)$; $\Delta\rho^2(r)$ is the convolution square of the scattering density contrast $\Delta\rho(r)$ averaged over all directions in space. $D_{\max}$ is the particle maximum dimension in such a way that $p(r)$ is zero for $r \geq D_{\max}$. In addition, the $p(r)$ function carries information about the scattering particle shape. In the ITP method, the $p(r)$ function is approximated by a sum of cubic B-spline functions. Only the main ideas are emphasized here and the reader is referred to the original papers for a more detailed description.

As an extension of the method, also developed by Glatter [28], the electron density distribution function $\rho(r)$ of particles with spherical, cylindrical, and lamellar symmetry can be obtained from $p(r)$ via the convolution square-root method (Decon program). Similarly to the $p(r)$ function, the $\rho(r)$ function is approximated by a series of N step functions (for details, see [28,29]). The Decon program generates the $\rho(r)$ function correlated with a $\bar{p}(r)$ which best agrees with the $p(r)$ function generated by the ITP program. If the chosen particle symmetry deviates from the actual one, the $\bar{p}(r)$ function is a poor approximation of the input $p(r)$ function [28].

From the micellar maximum dimension values, $D_{\max}$, obtained from the $p(r)$ curves, it is possible to calculate the anisotropy ν of spheroidal micellar aggregates, the ratio between the longest and the smallest axes, as:

$$\nu = \frac{D_{\max}}{2(R_{\mathrm{ef}} + \sigma)} \quad (2)$$

In the case of SLS micelles, an effective radius of the paraffinic medium is calculated as $R_{\mathrm{ef}} = (1-x)16.7+x17.6$ (where 16.7 Å and 17.6 Å correspond, respectively, to the extended dodecyl chain [30] and the TTC's hydrophobic extension (Santin Filho, O., personal communication); x is the anesthetic molar fraction and σ is the polar shell thickness.

From ν values one can calculate the volume of the SLS micelle polar shell (V_{pol}) and, consequently, the electron density distribution of the shell (ρ_{pol}) as:

$$\rho_{\mathrm{pol}} = \frac{\bar{n}_{\mathrm{SLS}}\, n_{\mathrm{e}}(\mathrm{SO_4Na}) + \bar{n}_{\mathrm{TTC}}\, n_{\mathrm{e}}(\mathrm{HN(CH_3)_2}) + NH\,\bar{n}\, n_{\mathrm{e}}(\mathrm{H_2O})}{V_{\mathrm{pol}}} \quad (3)$$

where $\bar{n}_{\mathrm{SLS}}$ is the SLS aggregation number; in the absence of TTC, $\bar{n}_{\mathrm{SLS}} v_1 = 4/3\pi v_{\mathrm{par}}(16.7)^3$ where v_1 is the volume of the hydrocarbon portion of SLS (350 Å^3 [30]) and v_{par} is the paraffinic anisotropy; $\bar{n}_{\mathrm{TTC}} = M_{\mathrm{TTC}}\ \bar{n}_{\mathrm{SLS}}$ is the TTC aggregation number; $\bar{n} = \bar{n}_{\mathrm{SLS}} + \bar{n}_{\mathrm{TTC}} = \bar{n}_{\mathrm{SLS}}(1+M_{\mathrm{TTC}})$ is the total aggregation number; NH is the number of water molecules per monomer; $n_{\mathrm{e}}(\mathrm{SO_4Na}) = 59$, $n_{\mathrm{e}}(\mathrm{HN(CH_3)_2}) = 26$ and $n_{\mathrm{e}}(\mathrm{H_2O}) = 10$ are, respectively, the number of electrons of the SLS headgroup, of the aliphatic amino group of TTC, and of water.

Once the total aggregation number $\bar{n}$ is obtained, one can calculate the mean cross-sectional area $\bar{a}$

through the following relationship:

$$\pi D_{max}^2/2 = \overline{n}.\overline{a} \quad (4)$$

3.2. EPR

The shapes of molecules (inverted cones) that favor micelle formation, as well as their organization in these approximately spherical aggregates lead to systems where the components are not tightly packed (the lateral pressure in these systems corresponds to 10 N/cm [31]). This loose packing allows for the contribution of various kinds of motion to the EPR spectral lineshapes of lipid spin probes in the micellar aggregates: probe rotation about its long molecular axis, intramolecular segmental motion (in the case of alkyl chains) [32–34], diffusion of the probe long molecular axis [35], and rotational diffusion of the micelle itself [34].

Although the molecular organization in a micelle implies a certain degree of order, the EPR spectra of an intercalated spin probe do not tend to display inner and outer extrema that allow the calculation of the order parameter [36]. Instead, often these spectra present three reasonably narrow lines, similar to those observed for isotropic motion, and, for this reason, they have been referred to as corresponding to pseudoisotropic motion [32–34]. Such features indicate that the spectral lineshapes are mostly determined by intra-micellar motion and orientation. Therefore, the EPR spectra of 5-MeSL in the systems studied in the present work will be discussed in terms of organizational properties of the micellar molecular components within the aggregates. Because it is not strongly anchored at the membrane–water interface, the probe was also found to exhibit pseudoisotropic motion in phospholipid bilayers [18]. Its spectra were analyzed in terms of an empirical parameter, h_{+1}/h_0 (the ratio of the heights of the low-field to the mid-field resonances), which contains the contribution of both order and mobility. Lower h_{+1}/h_0 values correspond to either higher order, or lower mobility, or both. We use the term organization to refer to the sum of both contributions [18].

3.3. Fluorescence

Binding of TTC to the micelles was assessed by changes in fluorescence intensity and maximum emission wavelength (λ_{em}).

4. Results

4.1. Fluorescence studies

The apparent pK, pK_{app}, of ionizable compounds is altered upon binding to model membrane systems; ΔpK is a function of both solute and surface charge [19].

For compounds that ionize according to the equilibrium

$$AH^+ \rightleftarrows A : + H^+,$$

pK_{app} is expected to decrease in the presence of a zwitterionic interface and to increase in the presence of a negatively charged interface. Such effects are a consequence of the difference between the binding constants of both forms: in the presence of a zwitterionic interface, the binding constant of the neutral form of a solute is greater than that of the cationic form, while the opposite is true in the presence of a negatively charged interface [19].

Thus, we determined pK_{app} for TTC in the presence of micellar HPS and SLS.

Fig. 1 shows that the fluorescence intensity of TTC increases as a function of pH in the presence of both SLS and HPS, albeit to a different extent. The lower intensity in the presence of SLS is probably due to a quenching, since the surfactant has been found to quench the fluorescence of some compounds. The experimental and calculated titration curves show that the pK of TTC changed from 8.26 in water [17] to 7.0 and 9.3 in the presence of HPS and SLS micelles, respectively, in good agreement with the expected pK changes and with results found for TTC in the same [17,20] or similar [18] systems.

The value of Δp$K = 1$ in the presence of SLS indicates that the binding constant of charged TTC is greater than that of the neutral form. Previous fluorescence measurements by Desai et al. [20] showed that at 20 mM SLS, both forms of TTC are totally bound. Therefore, at 35 mM detergent (used in the present case), the drug should be essentially totally bound to the micelle. Thus, the increase in fluorescence with increasing pH (Fig. 1) is due to the bind-

ing of the neutral drug to an environment of lower polarity.

Conversely, in the case of HPS, $\Delta pK = -1.3$ is an indication that neutral TTC binds more strongly than the cationic drug, in agreement with the values of $(3 \pm 1)10^3$ M^{-1} and $(0.10 \pm 0.05)10^3$ M^{-1} for their respective binding constants, K_b [37]. One can convert these constants into partition coefficients (P) [22], making use of the expression $P = K_b/V_p$ (where V_p is the detergent partial molar volume, 0.36 l mol^{-1}), and calculate that, under the present conditions, 74 and 99% of the LA bind to HPS at pH 4.5 and 10.0, respectively. Thus, the observed increase in fluorescence intensity at higher pH is due both to enhanced binding and, very likely (see below), to the uncharged form being located in an environment of lower polarity.

The maximum emission wavelength, λ_{em}, decreased from 373 nm for TTC in water [37] to 358 and 355 nm in the presence of SLS and HPS micelles, respectively, and remained constant during the pH titration. The decrease in λ_{em} is also an indication that the anesthetic bound to the micelles, experiencing an environment of lower dielectric constant [37].

The titration experiments allowed the choice of appropriate pHs for the EPR and SAXS measurements in order to investigate the effects of binding of charged and uncharged TTC on molecular organization, shape, and size of both micellar systems.

4.2. EPR studies

Fig. 2 exhibits EPR spectra of 5-MeSL in SLS micelles in the absence and presence of protonated (pH 6.5) and neutral (pH 12.0) TTC. They resemble reported spectra of the probe in micellar aggregates [32–34].

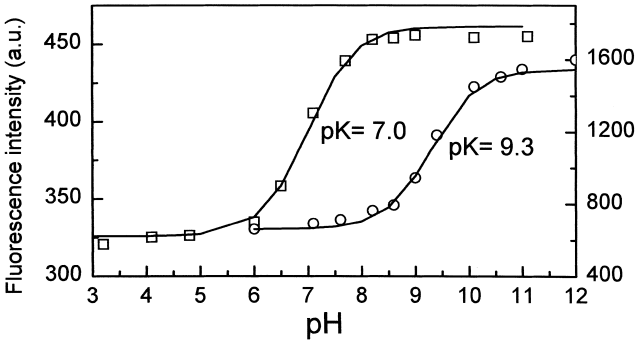

Fig. 1. Fluorescence intensity of 3 μM TTC as a function of pH in the presence of: (○) 1% (w/w) (35 mM) SLS; (□) 1% (w/w) HPS (25 mM). (—) theoretical fittings according to the Henderson–Hasselbalch equation.

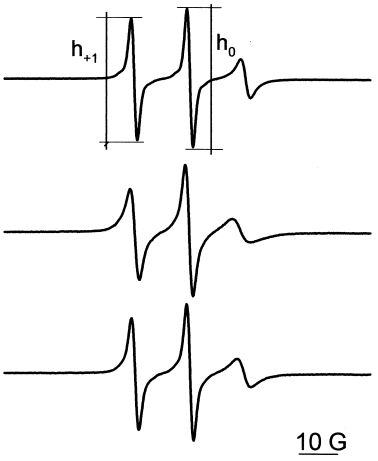

Fig. 2. EPR spectra of 5-MeSL incorporated in 1% (w/w) SLS at pH 6.5 (top and middle) and 12 (bottom). [TTC] = 0 (top) and 15 mM (middle and bottom). The figure shows how h_{+1} and h_0 were measured for the calculation of the h_{+1}/h_0 ratio.

Calculation of the h_{+1}/h_0 ratios for these spectra indicates that essentially no change in the molecular organization occurs within SLS micelles up to $M_{TTC} = 0.10$ (Fig. 3). For higher LA concentrations, the h_{+1}/h_0 ratio decreased at both pHs, the effect being greater for protonated (13%) than for neutral (4%) TTC at $M_{TTC} = 0.30$. The data suggest an increase in intramicellar organization upon binding of charged and, to a lesser extent, of uncharged TTC.

Since the spectra of 5-MeSL report on the region close to the micellar–aqueous interface, the above data indicated that cationic TTC has a stronger influence on molecular organization near the polar–apolar interface of SLS micelles.

Fig. 4 presents the h_{+1}/h_0 ratios obtained for HPS micelles. At pH 10.0 the TTC–HPS system precipitates even at low anesthetic concentrations. For this reason, the h_{+1}/h_0 ratio at pH 10.0 is given only for HPS in the absence of TTC. The spectral linewidths (Fig. 4, insert) are broader than in SLS, indicating a higher molecular organization in HPS. In the absence of TTC, the h_{+1}/h_0 ratio is 0.87 in SLS (Fig. 3), and 0.66 in HPS (Fig. 4).

In contrast with the findings for SLS, although 74% of protonated TTC was incorporated into the HPS micelles, the anesthetic did not significantly

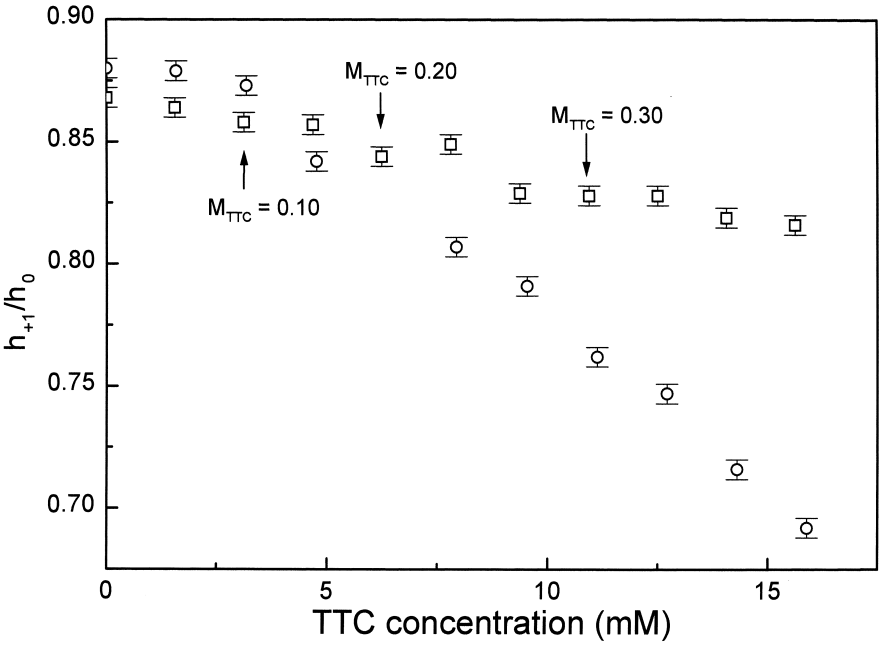

Fig. 3. h_{+1}/h_0 ratio in the EPR spectra of 5-MeSL incorporated in 1% (w/w) SLS as a function of TTC concentration at pH 6.5 (○) and 12.0 (□).

affect the molecular organization near the polar shell, since only a slight increase of h_{+1}/h_0 was observed (Fig. 4). Charged TTC was also found to have a small effect on zwitterionic egg phosphatidylcholine bilayers by spin labeling EPR [18].

4.3. SAXS studies

The scattering curves for micelles at increasing TTC concentrations are presented in Fig. 5a (pH 6.5) and Fig. 5b (pH 12.0). The corresponding distance distribution functions $p(r)$ are shown in Figs. 6a and 7a and the micelle maximum dimensions, D_{max}, are given in Table 1. While a significant change of the $p(r)$ function occurred at pH 6.5 and D_{max} increased between $M_{TTC} = 0.10$ and 0.20, at pH 12.0 both $p(r)$ and D_{max} remained essentially unaltered.

The SLS micelle electron density profile was determined by assuming spherical symmetry and using a five equidistant steps model (Figs. 6b and 7b). The $\rho(r)$ values provided by the program are arbitrary and were normalized considering the CH_3 group electron density (0.167 e/Å^3) and the water electron density ($\rho_w = 0.327$ e/Å^3). Fig. 6a and 7a present the best fittings of the $\bar{p}(r)$ functions (as calculated by the Decon program) to the $p(r)$ functions retrieved from the experimental curves (ITP program). The good agreement between both functions indicates that the micelles kept spherical symmetry with increasing anesthetic concentration.

The electron density levels did not change upon

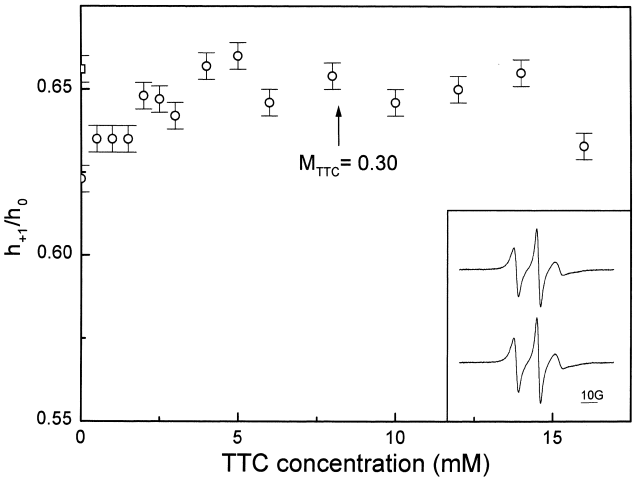

Fig. 4. h_{+1}/h_0 ratio in the EPR spectra of 5-MeSL incorporated in 1% (w/w) HPS as a function of TTC concentration at pH 4.5 (○) and 10.0 (□). Inset: EPR spectra of 5-MeSL incorporated in 1% (w/w) HPS micelles at 0 and 16.0 mM TTC (bottom), pH 4.5.

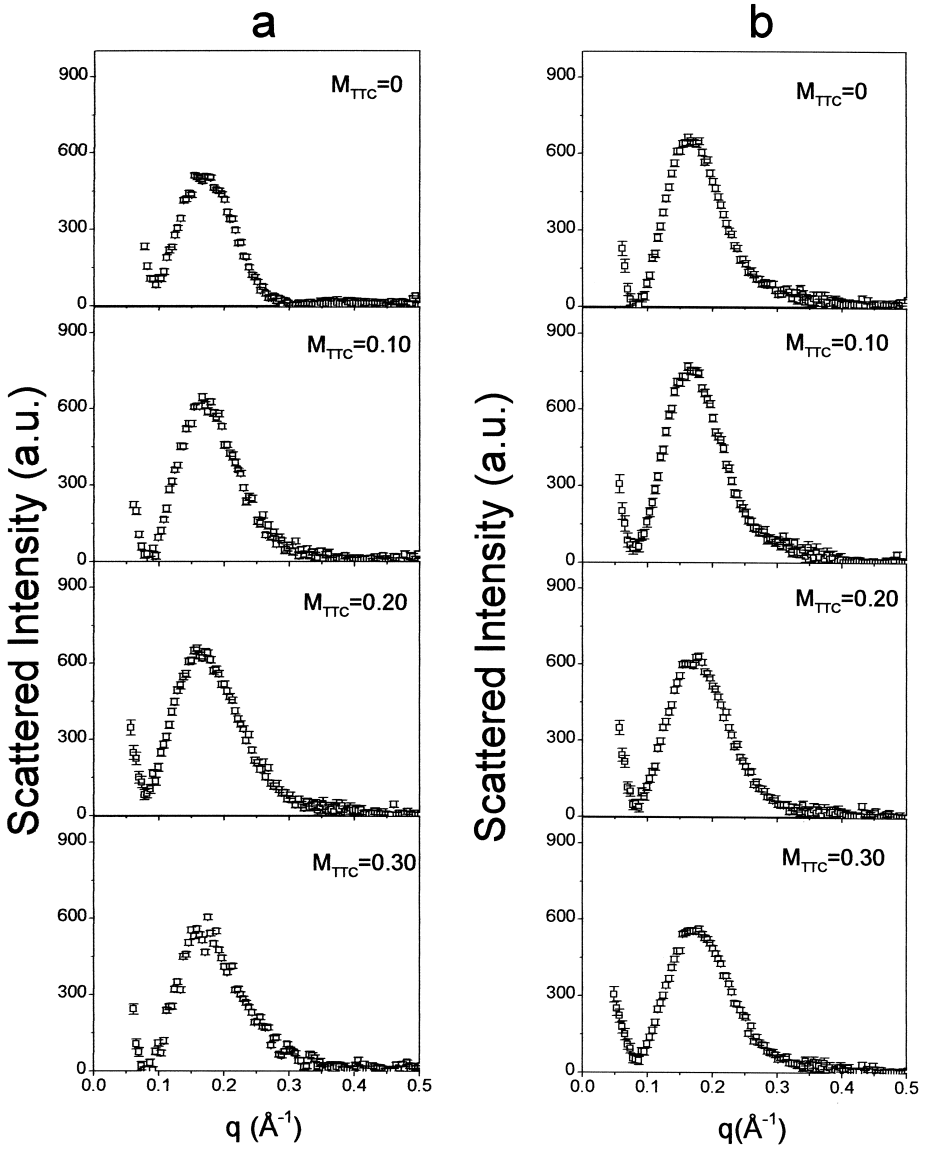

Fig. 5. SAXS curves for 1% (w/w) SLS/water as a function of TTC concentration, pH 6.5 (a) and 12.0 (b).

varying the TTC amount (Figs. 6b and 7b). Since the paraffinic electron density (ρ_{par}) is lower than the water electron density (ρ_w) and the polar shell density (ρ_{pol}) is higher than ρ_w, one can estimate the paraffinic region extension (the boundary between the non-polar and the hydrated polar shell) R_{par} to be the point where $\rho(r)$ intersects with ρ_w. Following this procedure, values of $R_{par} = 16 \pm 2$ Å were obtained, in full agreement with the effective radius R_{ef}.

A micellar anisotropy, $\nu = 1.43 \pm 0.05$, obtained from $D_{max} = 61 \pm 2$ Å (Table 1), according to Eq. 2, by assuming 4.6 Å as the thickness σ of the polar shell [38], indicates that in the cases of absence of drug, for M_{TTC} up to 0.10 of charged TTC, and for all concentrations of the uncharged LA, the SLS micelles are prolate ellipsoids, in good agreement with previous results in the absence of anesthetic [23]. Moreover, an average polar electron density (ρ_{pol}) of 0.35 e/Å^3 (Figs. 6b and 7b) is compatible with a polar shell containing ca. six water molecules per SLS monomer (Eq. 3), in the absence of LA, with an aggregation number $\bar{n}$ of 94 and a

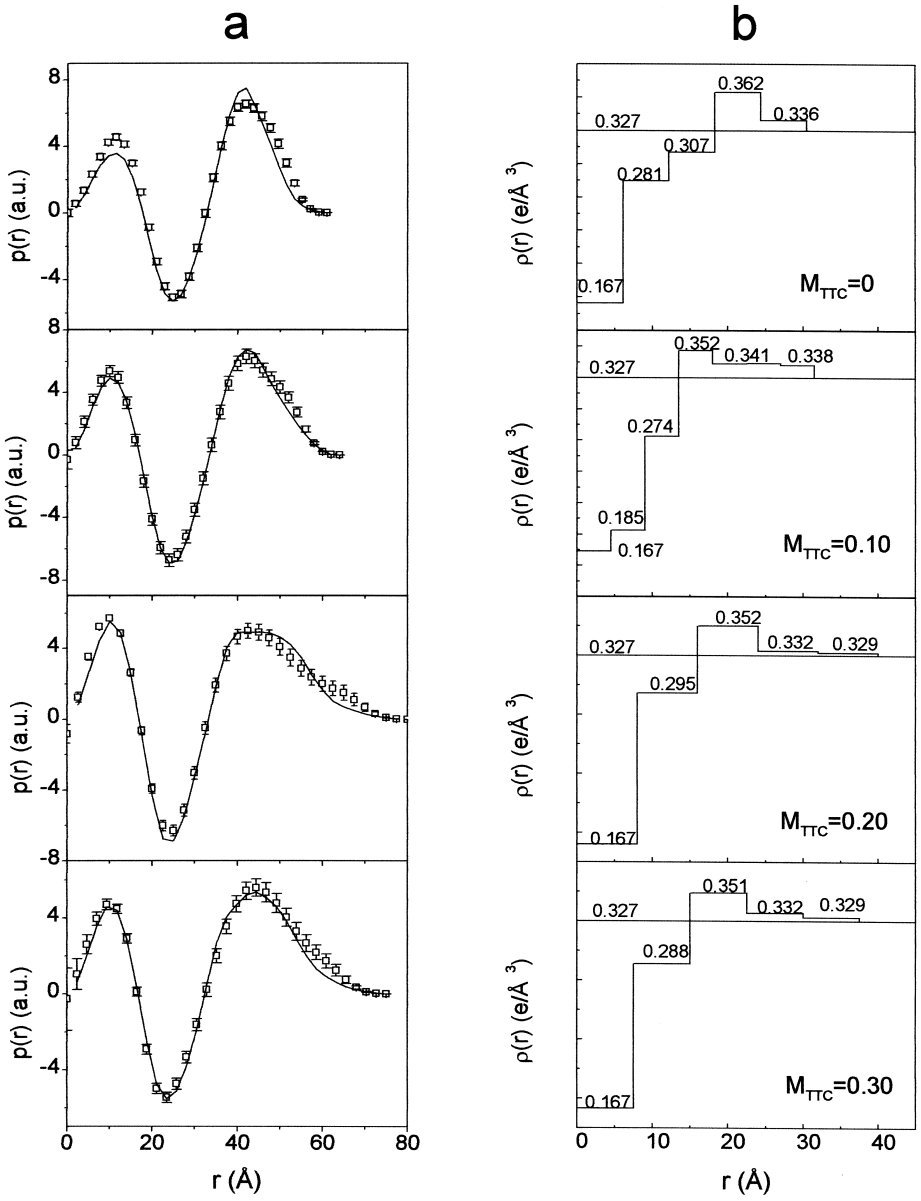

Fig. 6. (a) Distance distribution functions $p(r)$ of systems containing 1% (w/w) SLS/water in the presence of increasing TTC concentration at pH 6.5 (□); $\overline{p}(r)$ obtained theoretically by the Decon program (—). (b) Electron density distribution profile corresponding to the $\overline{p}(r)$ functions (Decon). For $M_{TTC} = 0.10$, seven electron density steps were used in order to get a better defined crossover from the paraffinic to the polar region.

mean area per SLS headgroup of 62 Å^2 (Eq. 4), in agreement with the literature [39].

For $M_{TTC} = 0.20$ of charged LA, D_{max} increased to 75 Å. This increase was verified by trying to fit the data with other D_{max} values, without satisfactory results. At the same time, greater D_{max} values were tried for $M_{TTC} = 0.10$, also without success. Therefore, there is a considerable increase in D_{max} ($\sim$23%) between $M_{TTC} = 0.10$ and 0.20. By taking into account that $\rho_{pol} = 0.35$ e/Å^3 remained the same upon TTC addition (Fig. 6b) and making use of Eq. 2 with a shell thickness of 4.6 Å, a value of $\nu = 1.75$ is obtained, which leads to $\overline{n} = 94$ for NH = 6 water molecules per monomer and a cross-sectional area $\overline{a}$ of 94 Å^2 (Eqs. 3 and 4). Obviously, the latter value is physically impossible due to micellar geomet-

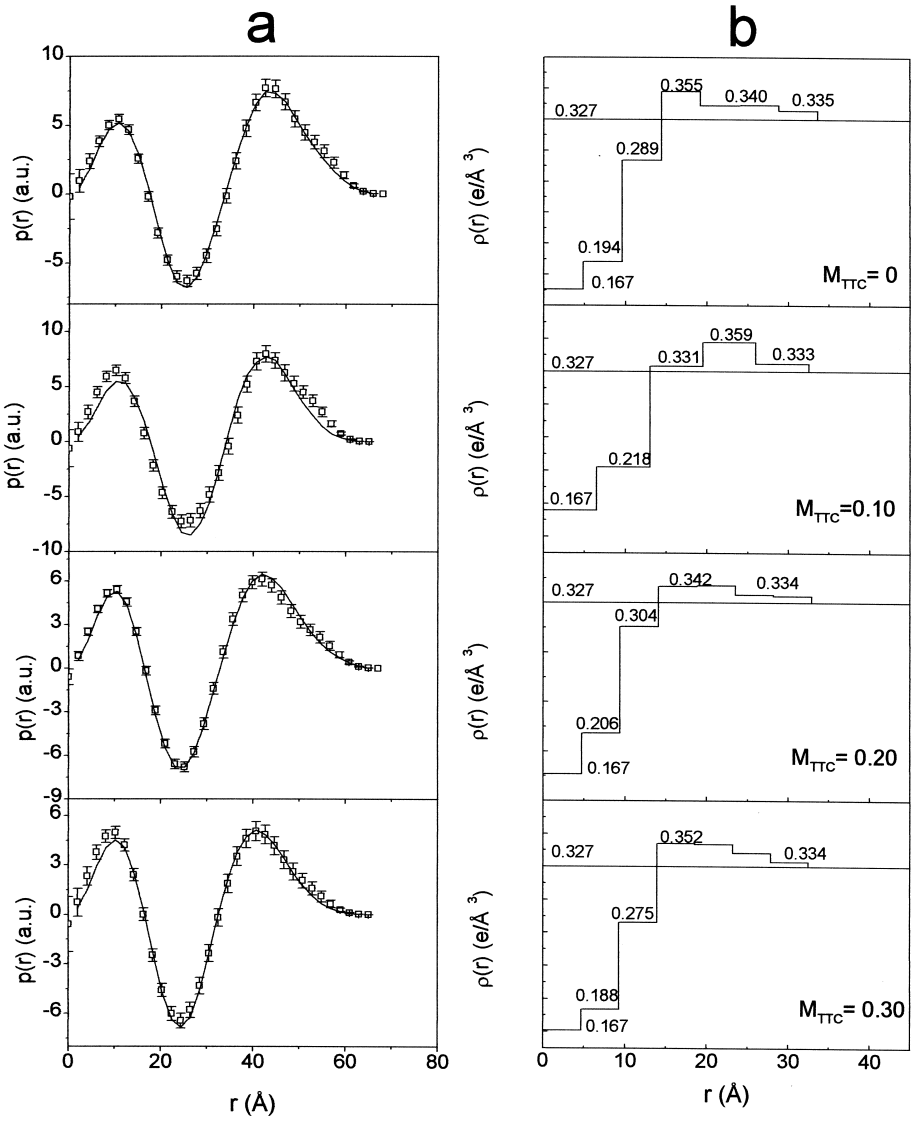

Fig. 7. (a) Distance distribution functions $p(r)$ of systems containing 1% (w/w) SLS/water in the presence of increasing TTC concentration at pH 12.0 (□); $\overline{p}(r)$ obtained theoretically by the Decon program (—). (b) Electron density distribution profile corresponding to the $\overline{p}(r)$ functions (Decon).

rical packing constraints [39]. If we consider a greater number of water molecules in the shell, $\overline{a}$ increases even more. On the other hand, if the micellar anisotropy remained invariable ($\nu = 1.43$) upon incorporation of protonated TTC, the polar shell thickness σ would have to increase to ca. 9 Å (Eq. 2), which is compatible with the electron density maps (Fig. 6b). With this assumption, $\overline{a} = 42$ Å^2 for $N\mathrm{H} = 6$ and $\overline{n} = 212$ (Eqs. 3 and 4). This value of $\overline{a}$ is too small; it is comparable to that observed in lamellar systems [39]. In contrast, for $N\mathrm{H} = 10$ and 12, $\overline{a} = 56$ Å^2 and 63 Å^2 ($\overline{n} = 157$ and 139), respectively. Therefore, a small decrease in the hydration number decreases the mean cross-sectional area per monomer.

For $M_{\mathrm{TTC}} = 0.30$ of the charged LA, $D_{\max}$ remains practically unaltered (Fig. 6 and Table 1), within the experimental uncertainties, leading to, for $\nu = 1.4$ and $8 \leq N\mathrm{H} \leq 10$, $\overline{a}$ values between 54 and 61 Å^2.

The SAXS curves for HPS (data not shown) are similar to those for SLS micelles. The corresponding $p(r)$ and $\rho(r)$ functions in the absence and presence of TTC and the $D_{\max}$ values are given in Fig. 8 and Table 1, respectively. Within the estimated errors, neither $p(r)$ nor $D_{\max}$ underwent alterations upon

Table 1
Micellar maximum dimension (D_{max}) obtained from the $p(r)$ functions of the systems containing 1% (w/w) SLS/water and 1% (w/w) HPS/water, for varying TTC concentration

Surfactant	pH	M_{TTC}	D_{max} (±2) (Å)
SLS	6.5	0	59
		0.10	61
		0.20	75
		0.30	70
	12	0	63
		0.10	62
		0.20	63
		0.30	63
HPS	4.5	0	82
		0.30	77

The error bars were estimated from the plots by dividing D_{max} by the number of points in the $p(r)$ curve, which yielded the interval (in Å) occupied by each point.

incorporation of the drug. The good agreement between the $p(r)$ and $\bar{p}(r)$ functions shows that the micelles are also spherically symmetric.

The electron density profiles were not altered upon addition of protonated TTC. From the electron density profiles (Fig. 8) a paraffinic radius $R_{par} = 21 \pm 3$ Å was determined, in good agreement with that estimated by Baptista et al. [40]. Considering the thickness of the hydrating shell around the bipolar region including the sulfonate anions as ca. 10 Å, and compared with the D_{max} value (Table 1), the HPS micelles, at these concentrations, are spheroids of low anisotropy.

5. Discussion

The changes in fluorescence intensity and in λ_{em} provided evidence for the incorporation of both

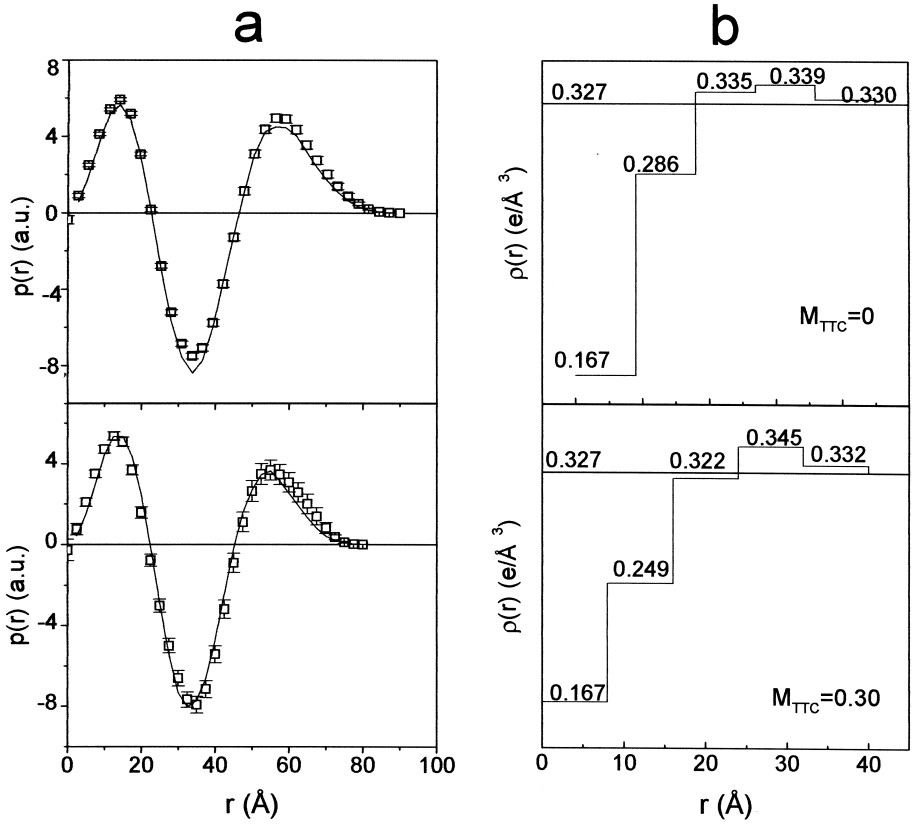

Fig. 8. (a) Distance distribution functions $p(r)$ of systems containing 1% (w/w) HPS/water at pH 4.5 for $M_{TTC} = 0$ and 0.30 (□); $\bar{p}(r)$ obtained theoretically by the Decon program (—). (b) Electron density distribution profile corresponding to the $\bar{p}(r)$ functions (Decon).

forms of TTC into anionic as well as zwitterionic detergent aggregates. In both cases, fluorescence intensity increased with increasing pH, suggesting that the uncharged form of the anesthetic must be located more deeply in the hydrocarbon region. In addition, it was possible to estimate that under the conditions used in the EPR and SAXS experiments essentially all the drug was bound to SLS micelles, both at low and high pH, whereas 74 and 99% of charged and uncharged TTC, respectively, were bound to HPS micelles.

The calculation of rotational correlation times from the EPR spectra of 5-MeSL according to the formalism of Kivelson [41], assuming pseudoisotropic motion, yields values of 0.93 ns and 3.3 ns in SLS in the absence and presence of TTC ($M_{TTC} = 0.30$) at pH 6.5, respectively, and of 5.0 ns in HPS both in the absence and in the presence of the anesthetic. In contrast, similar calculations making use of the Stokes–Einstein equation for the SAXS data yield, respectively, 24 ns and 48 ns for SLS at pH 6.5 in the absence and presence of the LA, and 58 ns for HPS both in the absence and in the presence of TTC. Both sets of values differ by one order of magnitude, indicating that the EPR spectral lineshapes are mostly determined by the motional and organizational properties of the micelle constituents. Thus, while the EPR studies yielded information about the effects of the LA–detergent interaction upon the organizational properties within the micellar aggregates, the SAXS data reported on properties of the whole particles, such as size and shape.

In this context, in the case of SLS micelles, the EPR spectra showed that, while addition of the cationic anesthetic increased the molecular organization close to the charged surface of the SLS micelles, binding of the uncharged LA had a much less pronounced effect. These results provide additional support for the conclusion that uncharged TTC is located more deeply in the micelle than its charged counterpart.

The electrostatic interaction between the positively charged TTC and the negatively charged SLS causes a decrease in the repulsive forces between the detergent molecules. This phenomenon should diminish the optimum area per head group, bringing about an increased molecular packing at the micellar surface. Taking this event into account, geometrical calculations showed that the most compatible interpretation of the SAXS results implies, for $M_{TTC} \geq 0.10$, an increase in micellar polar shell thickness, hydration number, and aggregation number, without much of an effect on the aggregate anisotropy. Since the increase in the polar shell thickness is accompanied by an increase in molecular organization within the aggregate, the hydration number must be such that the mean cross-sectional area is reduced due to the presence of the protonated LA in the anionic SLS micellar system. It has been observed that, upon salt addition, the change in the balance of forces responsible for the self-association process leads the system to assemble as more elongated spheroidal or even cylindrical micelles [42]. However, the ions are located at the water–micelle interface, whereas charged TTC resides within the micelle, giving rise to an additional hydrophobic contribution to the anesthetic–detergent interaction. This could explain the different effects of both agents on micellar size and shape.

When analyzing the uncharged TTC–SLS system, in spite of the fact that the EPR results indicate an increase in the molecular organization of the aggregates (Fig. 3), the SAXS data do not reveal any change in the micellar dimensions (Fig. 7). The increased molecular organization is probably due to the structure of TTC, which is more rigid than that of SLS. The lack of electrostatic interactions and the greater hydrophobicity of the neutral drug contribute to its deeper penetration in the micelle hydrophobic core.

In a theoretical simulation of the interaction of TTC with membranes, making use of a water–membrane interface model, represented by a dielectric discontinuity, charge effects were analyzed through the method of images [43] (Ota, A. and Ito, A.S., unpublished data). It was found that, whereas neutral TTC crosses the interface very easily going to the membrane interior, the charged drug is accomodated close to the water–membrane interface.

The present results are analogous to those obtained in deuterium NMR studies that showed that, while charged TTC is localized in the bilayer polar region, altering the packing of the zwitterionic phospholipid head groups, uncharged TTC penetrates more deeply into the membrane [44]. However, while uncharged TTC decreased the molecular organiza-

tion in the bilayer [9,18,44], in the present study the neutral drug increased the organization of the micellar aggregate.

As for the HPS system at pH 4.5, although the fluorescence data indicated that 74% of protonated TTC was bound to 25 mM detergent, neither the SAXS nor the EPR measurements provided evidence for a significant effect of the charged LA upon the structure or the molecular organization of the HPS micelles. This could be explained in terms of a more exposed location of the anesthetic due to the lack of a significant electrostatic interaction between the zwitterionic HPS headgroup and cationic TTC.

In conclusion, the combined use of fluorescence, EPR and SAXS provided a very detailed description of the effects of binding of the ionizable LA TTC to micellar aggregates.

From the point of view of the drug, binding to the micelles causes a change in its degree of ionization; as for the aggregates, information was obtained regarding the location of the charged and uncharged forms of the ligand, as well as the effects of binding on intra-micellar molecular organization. Finally, the consequences of binding on micellar mesoscopic properties were also evaluated.

The ability of LA to induce changes in packing and phase changes in model systems has been correlated with their pharmacological and toxic effects (see [4]). The information obtained in the present study should be of value for the understanding of these effects at the molecular level.

Acknowledgements

We thank the National Laboratory of Synchrotron Light (LNLS, Campinas, Brazil) for the use of their facility. This work was supported by research grants from FAPESP to S.S. and R.I., CAPES for a Ph.D. fellowship to C.V.T., FAPESP for a M.Sc. fellowship to F.C., and CNPq for research fellowships to S.S. and R.I.

References

[1] B. Hille, Prog. Biophys. Mol. Biol. 21 (1970) 3–32.
[2] L.D. van Dam, in: G.R. Strichartz (Ed.), Local Anesthetics, vol. 81, Springer-Verlag, Berlin, 1987, pp. 1–20.
[3] B.G. Covino, in: G.R. Strichartz (Ed.), Local Anesthetics, vol. 81, Springer-Verlag, Berlin, 1987, pp. 187–212.
[4] E. de Paula, S. Schreier, Braz. J. Med. Biol. Res. 29 (1996) 877–894.
[5] P.R. Cullis, A.J. Verkleij, Biochim. Biophys. Acta 552 (1979) 546–551.
[6] A.P. Hornby, P.R. Cullis, Biochim. Biophys. Acta 647 (1981) 285–292.
[7] M.F. Fernandez, Biochim. Biophys. Acta 597 (1980) 83–91.
[8] M.F. Fernandez, Biochim. Biophys. Acta 647 (1981) 27–30.
[9] W.A. Frezatti Jr., W.R. Toselli, S. Schreier, Biochim. Biophys. Acta 860 (1986) 531–538.
[10] A.G. Lee, Nature 262 (1976) 545–548.
[11] J.R. Trudell, Anesthesiology 46 (1977) 5–10.
[12] F.W. Co Tui, A.L. Preiss, I. Barcham, M.I. Nevin, J. Pharm. Exp. Ther. 81 (1944) 209–217.
[13] M.D. Sokoll, B. Sonesson, S. Thesleff, Eur. J. Pharmacol. 4 (1968) 179–187.
[14] H.J. Adams, A.R. Mastri, A.W. Eicholzer, G. Kilpatrick, Anesthesia Analg. 53 (1974) 904–908.
[15] M. Boljka, G. Kolar, J. Vidensek, Br. J. Ophthalmol. 78 (1994) 386–389.
[16] A.G. Lee, Biochim. Biophys. Acta 448 (1976) 34–44.
[17] J. Garcia-Soto, M.S. Fernández, Biochim. Biophys. Acta 731 (1983) 275–281.
[18] S. Schreier, W.A. Frezzatti Jr, P.S. Araujo, H. Chaimovich, I.M. Cuccovia, Biochim. Biophys. Acta 769 (1984) 231–237.
[19] A.G. Lee, S. Schreier, in: G. Gregoriadis (Ed.), Liposome Technology, vol. II, CRC, Boca Raton, FL, 1993, 1–25.
[20] S. Desai, T. Hadlock, C. Messani, R. Chafitz, G. Strichartz, J. Pharmacol. Exp. Ther. 271 (1994) 220–228.
[21] M.L. Bianconi, A.T. Amaral, S. Schreier, Biochem. Biophys. Res. Commun. 152 (1988) 344–350.
[22] M.L. Bianconi, S. Schreier, J. Phys. Chem. 95 (1991) 2483–2487.
[23] R. Itri, L.Q. Amaral, Phys. Rev. E47 (1993) 2551–2557; Erratum in E58 (1998) 1173–1174.
[24] R. Itri, L.Q. Amaral, J. Phys. Chem 95 (1991) 423–427.
[25] R. Itri, L.Q. Amaral, J. Appl. Cryst. 27 (1994) 20–24.
[26] O. Glatter, Acta Phys. Aust. 47 (1977) 83–102.
[27] O. Glatter, J. Appl. Cryst. 10 (1977) 415–421.
[28] O. Glatter, J. Appl. Cryst. 14 (1981) 101–108.
[29] O. Glatter, J. Appl. Cryst. 17 (1984) 435–441.
[30] C. Tanford, J. Phys. Chem. 76 (1972) 3020–3024.
[31] A. Seelig, Biochim. Biophys. Acta 884 (1987) 196–204.
[32] J.R. Ernandes, S. Schreier, H. Chaimovich, Chem. Phys. Lipids 16 (1976) 19–30.
[33] J.R. Ernandes, H. Chaimovich, S. Schreier, Chem. Phys. Lipids 18 (1977) 304–315.
[34] S. Schreier, J.R. Ernandes, I.M. Cuccovia, H. Chaimovich, J. Magn. Res. 30 (1978) 283–298.
[35] Z. Liang, P. Westlund, G. Wikander, J. Chem. Phys. 99 (1993) 7098–7107.

[36] S. Schreier, C.F. Polnaszeck, I.C.P. Smith, Biochim. Biophys. Acta 515 (1978) 375–436.
[37] G.S.S. Ferreira, D.M. Périgo, M.J. Politi, S. Schreier, Photochem. Photobiol. 63 (1996) 755–761.
[38] D. Stigter, J. Phys. Chem. 68 (1964) 3603–3611.
[39] H. Wennerström, B. Lindmann, Phys. Rep. 52 (1979) 1–86.
[40] M.S. Baptista, I. Cuccovia, H. Chaimovich, M.J. Politi, J. Phys. Chem. 96 (1992) 6442–6449.
[41] D. Kivelson, J. Chem. Phys. 33 (1960) 1094–1106.
[42] P.J. Missel, N.A. Mazer, G.B. Benedek, C.Y. Young, M.C. Carey, J. Phys. Chem. 87 (1983) 1264–1277.
[43] P.G. Pascutti, E.P.G. Areas, A.S. Ito, K.C. Mundin, P.M. Bisch, Prog. Biophys. Mol. Biol. PA 65 (1996) 340.
[44] Y. Boulanger, S. Schreier, I.C.P. Smith, Biochemistry 20 (1981) 6824–6830.